

Quantum radiation generated by a moving mirror in free space

P. A. Maia Neto

Instituto de Física, Universidade Federal do Rio de Janeiro, Caixa Postal 68528, 21945-970 Rio de Janeiro, Rio de Janeiro, Brazil

L. A. S. Machado

Departamento de Física, Pontifícia Universidade Católica do Rio de Janeiro, Caixa Postal 38071, 22452 Rio de Janeiro, Rio de Janeiro, Brazil

(Received 22 April 1996)

We consider a single perfectly reflecting plane mirror moving in the vacuum of the electromagnetic field, in the nonrelativistic approximation. We calculate the frequency and angular spectra of the emitted radiation. Photons are created in pairs, implying some simple and general properties of the spectra. In the case of TM-polarized photons, the angular distribution is concentrated on a particular direction that depends on the photon frequency, whereas TE photons are smoothly distributed around the direction perpendicular to the surface of the mirror. The total radiated energy is shown to be related to the dissipative force exerted on the mirror, in agreement with energy conservation. [S1050-2947(96)09409-7]

PACS number(s): 42.50.Lc, 42.50.Dv, 03.65.-w, 12.20.Ds

I. INTRODUCTION

The most well-known illustration of mechanical effects related to the quantum vacuum field is the Casimir force between two mirrors at rest. A new effect appears when the mirrors are set to move. In this case, the vacuum field may exert a force that tries to damp the motion [1–3]. Such dissipative force may be understood as the mechanical effect of the emission of radiation induced by the motion of the mirror in vacuum. Pairs of photons are created out of the vacuum state, and energy conservation entails the existence of a radiation reaction force working against the motion.

The simplest theoretical model amounts to consider only propagation along the direction perpendicular to the plane of the mirror (one-dimensional or 1D models). Photon emission in the case of lossless 1D cavities with moving end mirrors was considered in Refs. [4,5]. A more complete treatment, taking into account a finite transmissivity through the mirrors, has been recently presented [6].

Recently, three-dimensional (3D) calculations were performed in several contexts, including dielectric media moving sideways [7,8], cavities with oscillating boundaries [9], and collapsing dielectric spheres [10] (the latter in connection with sonoluminescence). Emission of photons may occur even in the presence of a single moving mirror in vacuum, as shown in the context of 1D models [6,11]. In this paper, we calculate the spectra for photon emission considering the full 3D electromagnetic field. As a simple illustration, we take a plane perfectly reflecting mirror moving along the normal to its surface, which is taken to be the x direction. We neglect the recoil of the mirror due to photon emission. Accordingly, we assume that the mirror's position is a given function of time imposed by some external means:

$$x = \delta q(t).$$

Furthermore, we assume that $\delta q(t)$ corresponds to a bounded nonrelativistic motion: $\delta \dot{q}(t) \ll c$, where c is the speed of light. This last assumption entails that only low-

frequency photons are emitted, allowing us to employ simple analytical methods based on the long-wavelength approximation. The same model was considered by one of us in order to calculate the dissipative force exerted on the mirror [3]. Although the total radiated energy may be correctly obtained from the dissipative force through energy conservation [12], it is not possible to extract information about the photon spectra from it. Accordingly, here we employ a different approach, based on the manipulation of suitable Green functions, which turns out to be more convenient for the derivation of the photon spectra.

The paper is organized in the following way. In Sec. II, we derive the boundary conditions for the electromagnetic field, treating separately the two field polarizations and employing the long wavelength approximation. Output fields are then obtained in terms of input fields in Sec. III, allowing us to compute the rate of photon emission at a given frequency and spatial direction in Sec. IV. We discuss our results in Sec. V.

II. BOUNDARY CONDITIONS IN THE LONG WAVELENGTH APPROXIMATION

The condition of perfect reflectivity implies that the electromagnetic fields \mathbf{E}' and \mathbf{B}' measured in the instantaneously comoving Lorentz frame S' obey the boundary conditions [13]:

$$\hat{\mathbf{x}} \times \mathbf{E}'|_{\text{mirror}} = \mathbf{0}, \quad \hat{\mathbf{x}} \cdot \mathbf{B}'|_{\text{mirror}} = 0. \quad (1)$$

In order to solve the problem of scattering by a moving plane mirror, our first step is to decompose the input plane waves into components corresponding to the electric field parallel (TM) or perpendicular (TE) to the plane of incidence. Each polarization is then represented by carefully chosen potentials. We use mks units with $\epsilon_0 = 1$, $c = 1$.

For the TE field, we take the usual vector potential $\mathbf{A}^{(\text{TE})}$, defined through the equations

$$\mathbf{E}^{(\text{TE})} = -\partial_t \mathbf{A}^{(\text{TE})}, \quad \mathbf{B}^{(\text{TE})} = \nabla \times \mathbf{A}^{(\text{TE})}, \quad (2)$$

and which is taken in the Coulomb gauge: $\nabla \cdot \mathbf{A}^{(\text{TE})} = 0$. The key point in the derivation of the boundary condition for $\mathbf{A}^{(\text{TE})}$ is the property $\hat{\mathbf{x}} \cdot \mathbf{A}^{(\text{TE})} = 0$, which entails the invariance of $\mathbf{A}^{(\text{TE})}$ under the Lorentz boost from the comoving to the laboratory frame. As shown in Ref. [3], the condition resulting from Eqs. (1) and (2) is given by

$$\mathbf{A}^{(\text{TE})}(x = \delta q(t), y, z, t) = \mathbf{0}. \quad (3)$$

Equation (3) was first obtained by Moore [13] in the particular case of 1D models.

In the case of TM polarization, the vector potential defined as in Eq. (2) does have in general a component along the x direction, thus resulting in complicated boundary conditions. A much simpler approach was introduced in Refs. [3,14], which relies on the definition of a new vector potential $\mathcal{A}^{(\text{TM})}$ as

$$\mathbf{E}^{(\text{TM})} = \nabla \times \mathcal{A}^{(\text{TM})}, \quad \mathbf{B}^{(\text{TM})} = \partial_t \mathcal{A}^{(\text{TM})}. \quad (4)$$

Moreover, we choose the gauge given by $\nabla \cdot \mathcal{A}^{(\text{TM})} = 0$. As in the case of TE polarization, we have $\hat{\mathbf{x}} \cdot \mathcal{A}^{(\text{TM})} = 0$, hence yielding a simple boundary condition for $\mathcal{A}^{(\text{TM})}$ in the non-relativistic approximation (see Ref. [3]):

$$[\partial_x + \delta \dot{q}(t) \partial_t + O(\delta \dot{q}(t)^2)] \mathcal{A}^{(\text{TM})}(x, \mathbf{r}_{\parallel}, t)|_{x=\delta q(t)} = \mathbf{0}. \quad (5)$$

In the particular case of a *stationary* mirror, we may write a normal mode decomposition for the fields, which are then denoted as $\mathbf{A}_{\text{sta}}^{(\text{TE})}$ and $\mathcal{A}_{\text{sta}}^{(\text{TM})}$. We take periodic boundary conditions on the yz plane over a square of surface S , which is identified with the (very large) surface of the mirror. Then the components of the wavevectors parallel to the plane of the mirror are restricted to discrete values:

$$\mathbf{k}_{\parallel n} = \frac{2\pi}{\sqrt{S}} (n_y \hat{\mathbf{y}} + n_z \hat{\mathbf{z}}), \quad (6)$$

where the index n denotes a given pair of integer numbers (n_y, n_z) . We assume the mirror to be at $x=0$, and hence take $\delta q(t) = 0$ in Eqs. (3) and (5). For the TE field, we find

$$\begin{aligned} \mathbf{A}_{\text{sta}}^{(\text{TE})}(x, \mathbf{r}_{\parallel}, t) &= i \int_0^{\infty} \frac{dk_x}{2\pi} \sum_n \sqrt{\frac{2\hbar}{\omega_n S}} \sin(k_x x) \\ &\times e^{i\mathbf{k}_{\parallel n} \cdot \mathbf{r}_{\parallel}} e^{-i\omega_n t} a_n^{(\text{TE})}(k_x) \hat{\mathbf{x}} \times \hat{\mathbf{k}}_{\parallel n} + \text{H.c.}, \end{aligned} \quad (7)$$

with

$$\omega_n = \sqrt{k_x^2 + k_{\parallel n}^2} \quad (8)$$

and where H.c. means the Hermitian conjugate. The TM field is written as follows:

$$\begin{aligned} \mathcal{A}_{\text{sta}}^{(\text{TM})}(x, \mathbf{r}_{\parallel}, t) &= \int_0^{\infty} \frac{dk_x}{2\pi} \sum_n \sqrt{\frac{2\hbar}{\omega_n S}} \cos(k_x x) \\ &\times e^{i\mathbf{k}_{\parallel n} \cdot \mathbf{r}_{\parallel}} e^{-i\omega_n t} a_n^{(\text{TM})}(k_x) \hat{\mathbf{x}} \times \hat{\mathbf{k}}_{\parallel n} + \text{H.c.} \end{aligned} \quad (9)$$

The fields in Eqs. (7)–(9) are normalized so as to yield the following representation for the field Hamiltonian corresponding to the half-space $x \geq 0$:

$$\begin{aligned} H &= \sum_{\epsilon=\text{TE, TM}} \sum_n \int_0^{\infty} \frac{dk_x}{2\pi} \frac{\hbar \omega_n(k_x)}{2} \\ &\times [a_n^{\epsilon}(k_x)^{\dagger} a_n^{\epsilon}(k_x) + a_n^{\epsilon}(k_x) a_n^{\epsilon}(k_x)^{\dagger}]. \end{aligned} \quad (10)$$

The operators $a_n^{(\text{TM})}(k_x)$ and $a_n^{(\text{TE})}(k_x)$ obey the commutation relations

$$[a_n^{\epsilon}(k_x), a_{n'}^{\epsilon'}(k')] = 0 \quad (11)$$

and

$$[a_n^{\epsilon}(k_x), a_{n'}^{\epsilon'}(k')^{\dagger}] = 2\pi \delta(k_x - k') \delta_{n, n'} \delta_{\epsilon, \epsilon'}, \quad (12)$$

where $\epsilon = \text{TE, TM}$ stands for the polarization.

In order to consider the effect of the motion of the mirror, we write the fields as

$$\mathbf{A}^{(\text{TE})} = \mathbf{A}_{\text{sta}}^{(\text{TE})} + \delta \mathbf{A}^{(\text{TE})} \quad (13)$$

and

$$\mathcal{A}^{(\text{TM})} = \mathcal{A}_{\text{sta}}^{(\text{TM})} + \delta \mathcal{A}^{(\text{TM})}, \quad (14)$$

where $\delta \mathbf{A}^{(\text{TE})}$ and $\delta \mathcal{A}^{(\text{TM})}$ correspond to the field modification due to the mirror's motion. They are usually of the order of $\delta q(t)$, and hence represent a small perturbation of the motionless case. The only exception occurs in the case of TM polarization, when the parameters are such as to scatter radiation near the grazing direction [14]. Here we neglect this possibility and accordingly solve Eqs. (3) and (5) by taking a perturbative expansion. Furthermore, we assume that the fields are nearly constant over a distance of the order of $\delta q(t)$, and hence expand Eqs. (3) and (5) up to first order in $\delta q(t)$. As discussed in Sec. IV, the long-wavelength approximation is closely connected to the nonrelativistic limit as far as the photon emission effect is concerned. Replacing Eqs. (13) and (14) into Eqs. (3) and (5) yield

$$\delta \mathbf{A}^{(\text{TE})}(0, y, z, t) = -\delta q(t) \partial_x \mathbf{A}_{\text{sta}}^{(\text{TE})}(0, y, z, t) \quad (15)$$

and

$$\partial_x \delta \mathcal{A}^{(\text{TM})}(0, y, z, t) = -(\delta q(t) \partial_x^2 + \delta \dot{q}(t) \partial_t) \mathcal{A}_{\text{sta}}^{(\text{TM})}(0, y, z, t). \quad (16)$$

Equations (19) and (20) provide the first-order boundary conditions for the fields. They result from the long wavelength approximation as well as from assuming the motional corrections to be small perturbations.

In order to benefit from the plane symmetry, we Fourier transform the fields as follows:

$$\mathbf{A}_n^{(\text{TE})}[x, \omega] = \frac{1}{S} \int dt \int_S d^2 \mathbf{r}_{\parallel} e^{i\omega t} e^{-i\mathbf{k}_{\parallel n} \cdot \mathbf{r}_{\parallel}} \mathbf{A}^{(\text{TE})}(x, \mathbf{r}_{\parallel}, t), \quad (17)$$

where $\mathbf{r}_{\parallel} = (y, z)$ is the position on the surface of the mirror, and proceed likewise for $\mathcal{A}^{(\text{TM})}$. The mixed representation of

Eq. (17) differs from its reciprocal space analog used in Eqs. (7) and (9) by keeping the real space coordinate x . This is convenient for treating the scattering by the mirror, which is at a given time-dependent position along the x axis. Since $\mathbf{A}^{(\text{TE})}$ and $\mathcal{A}^{(\text{TM})}$ satisfy the wave equation, the two representations are closely connected. In fact, the variables $\mathbf{k}_{\parallel n}$ and ω define exactly two wave vectors \mathbf{k} , which are given by $\mathbf{k} = \pm k_x \hat{\mathbf{x}} + \mathbf{k}_{\parallel n}$ with

$$k_x = [(\omega + i\epsilon)^2 - k_{\parallel n}^2]^{1/2}, \quad \epsilon \rightarrow 0^+, \quad (18)$$

defined as a function of ω with a branch cut along the segment on the real axis between $-k_{\parallel n}$ and $k_{\parallel n}$. Here ω is an independent variable assuming both positive and negative values, whereas the frequency ω_n in Eq. (8) is positive defined.

In the Fourier representation defined by Eq. (17), the boundary conditions given by Eqs. (15) and (16) read

$$\delta \mathbf{A}_n^{(\text{TE})}[0, \omega] = - \int \frac{d\omega'}{2\pi} \theta(k_x'^2) \delta q[\omega - \omega'] \partial_x \mathbf{A}_{\text{sta}_n}^{(\text{TE})}[0, \omega'] \quad (19)$$

and

$$\begin{aligned} \partial_x \delta \mathcal{A}_n^{(\text{TM})}[0, \omega] = & - \int \frac{d\omega'}{2\pi} \theta(k_x'^2) \delta q[\omega - \omega'] \\ & \times (k_{\parallel n}^2 - \omega \omega') \mathcal{A}_{\text{sta}_n}^{(\text{TM})}[0, \omega'], \end{aligned} \quad (20)$$

where $\delta q[\omega]$ is the Fourier transform of $\delta q(t)$, k_x' is a function of $k_{\parallel n}$ and ω' as in Eq. (18), and $\theta(k_x'^2)$ is the step function of $k_x'^2$. Note that the same index n appears in both sides of Eqs. (19) and (20), corresponding to the property that $\mathbf{k}_{\parallel n}$ is conserved in the scattering by the mirror, as expected from plane symmetry. Accordingly, the scattering of $\mathbf{A}_n^{(\text{TE})}[x, \omega]$ provides vector fields all polarized along a fixed direction in space, given by the product $\hat{\mathbf{x}} \times \mathbf{k}_{\parallel n}$ (the same holding for TM polarization). Therefore, the scattering of the electromagnetic field by a plane boundary is reduced to two independent effective scalar problems, corresponding, according to Eqs. (19) and (20), to Dirichlet and Neumann boundary conditions. Their solutions are obtained in the next section.

III. INPUT AND OUTPUT FIELDS

In this section, we derive a linear transformation between output and input field operators. We start from Eqs. (13) and (14), and then use Dirichlet and Neumann Green functions, $G_D(x|x')$ and $G_N(x|x')$ in order to write

$$\mathbf{A}_n^{(\text{TE})}[x, \omega] = \mathbf{A}_{\text{sta}_n}^{(\text{TE})}[x, \omega] - \partial_x G_D(x|x'=0) \delta \mathbf{A}_n^{(\text{TE})}[x'=0, \omega] \quad (21)$$

and

$$\begin{aligned} \mathcal{A}_n^{(\text{TM})}[x, \omega] = & \mathcal{A}_{\text{sta}_n}^{(\text{TM})}[x, \omega] + G_N(x|x'=0) \\ & \times \partial_x \delta \mathcal{A}_n^{(\text{TM})}[x'=0, \omega], \end{aligned} \quad (22)$$

with $\delta \mathbf{A}_n^{(\text{TE})}[x=0, \omega]$ and $\delta \mathcal{A}_n^{(\text{TM})}[x'=0, \omega]$ given by Eqs. (19) and (20).

We assume that the motion takes place during a finite time interval. Then, if we take retarded Green functions (denoted by the superscript R) in Eqs. (21) and (22), which are such that

$$\partial_x G_D^R(x|x'=0) = -e^{ik_x|x|}, \quad G_N^R(x|x'=0) = ie^{ik_x|x|}/k_x, \quad (23)$$

and with k_x defined by Eq. (18), the stationary fields $\mathbf{A}_{\text{sta}}^{(\text{TE})}$ and $\mathcal{A}_{\text{sta}}^{(\text{TM})}$ in Eqs. (21) and (22) represent input fields, denoted as $\mathbf{A}_{\text{in}}^{(\text{TE})}$ and $\mathcal{A}_{\text{in}}^{(\text{TM})}$. They correspond to the total field in the limit $t \rightarrow -\infty$. On the other hand, when taking advanced Green functions, being such that

$$\begin{aligned} \partial_x G_D^A(x|x'=0) = & -e^{-ik_x^*|x|}, \\ G_N^A(x|x'=0) = & -ie^{-ik_x^*|x|}/k_x^*, \end{aligned} \quad (24)$$

the stationary fields are replaced by the output fields $\mathbf{A}_{\text{out}_n}^{(\text{TE})}$ and $\mathcal{A}_{\text{out}_n}^{(\text{TM})}$ in Eqs. (21) and (22), which correspond to the limit $t \rightarrow \infty$.

We consider the radiation emitted into the half space corresponding to the positive x axis, and accordingly assume $x \geq 0$ from now on. In order to derive the relation between input and output fields, we combine the retarded and advanced Green functions to write, from Eq. (21),

$$\begin{aligned} \mathbf{A}_{\text{out}_n}^{(\text{TE})}[x, \omega] = & \mathbf{A}_{\text{in}_n}^{(\text{TE})}[x, \omega] \\ & - [\partial_x G_D^R(x|x'=0) - \partial_x G_D^A(x|x'=0)] \\ & \times \delta \mathbf{A}_n^{(\text{TE})}[x'=0, \omega] + O(\delta q^2) \end{aligned} \quad (25)$$

and likewise we derive from Eq. (22),

$$\begin{aligned} \mathcal{A}_{\text{out}_n}^{(\text{TM})}[x, \omega] = & \mathcal{A}_{\text{in}_n}^{(\text{TM})}[x, \omega] \\ & + [G_N^R(x|x'=0) - G_N^A(x|x'=0)] \\ & \times \partial_x \delta \mathcal{A}_n^{(\text{TM})}[x'=0, \omega] + O(\delta q^2). \end{aligned} \quad (26)$$

In Eqs. (25) and (26) $\delta \mathbf{A}_n^{(\text{TE})}[0, \omega]$ and $\delta \mathcal{A}_n^{(\text{TM})}[0, \omega]$ are given by Eqs. (19) and (20) with the stationary fields replaced by the input fields. Then, from Eqs. (19) and (23)–(25) we derive for the TE fields

$$\begin{aligned} \mathbf{A}_{\text{out}_n}^{(\text{TE})}[x, \omega] = & \mathbf{A}_{\text{in}_n}^{(\text{TE})}[x, \omega] - 2i \sin(k_x x) \\ & \times \int \frac{d\omega'}{2\pi} \theta(k_x'^2) \delta q[\omega - \omega'] \partial_x \mathbf{A}_{\text{in}_n}^{(\text{TE})}[0, \omega'], \end{aligned} \quad (27)$$

a result valid to first order in δq . For the TM field, we use Eqs. (20) and (26) instead of Eqs. (19) and (25) and then find

$$\begin{aligned} \mathcal{A}_{\text{out}_n}^{(\text{TM})}[x, \omega] &= \mathcal{A}_{\text{in}_n}^{(\text{TM})}[x, \omega] - \frac{2i \cos(k_x x)}{k_x} \int \frac{d\omega'}{2\pi} \theta(k_x'^2) \\ &\times \delta q[\omega - \omega'](k_{\parallel n}^2 - \omega \omega') \mathcal{A}_{\text{in}_n}^{(\text{TM})}[0, \omega']. \end{aligned} \quad (28)$$

An important property of Eqs. (27) and (28) is the absence of evanescent wave components. This is expected, since evanescent waves are bounded near the mirror's surface, and hence do not contribute to radiation. Note however that both the retarded and advanced solutions of Eqs. (19) and (20) contain evanescent components, which are (exactly) subtracted away when computing the input-output relations from Eqs. (25) and (26).

We may get more physical insight on the input-output transformation by considering the field normal mode decomposition and then deriving a linear transformation for the annihilation and creation operators. We assume that the mirror was initially at $x=0$, and then after bouncing during a finite time interval it comes back to its original position. Thus, both output and input fields have the same normal mode decomposition as in Eqs. (7) and (9). We replace $\mathbf{A}_{\text{sta}}^{(\text{TE})}$ by $\mathbf{A}_{\text{in}}^{(\text{TE})}$ and $\mathcal{A}_{\text{sta}}^{(\text{TM})}$ by $\mathcal{A}_{\text{in}}^{(\text{TM})}$ and then Fourier transform the expressions in Eqs. (7) and (9) according to the rule defined by Eq. (17) to find

$$\begin{aligned} \mathbf{A}_{\text{in}_n}^{(\text{TE})}[x, \omega] &= i \theta(k_x^2) \sqrt{\frac{2\hbar|\omega|}{k_x^2 S}} \sin(k_x x) \\ &\times [\theta(\omega) a_{\text{in}_n}^{(\text{TE})}(k_x) - \theta(-\omega) a_{\text{in}_{-n}}^{(\text{TE})}(-k_x)^\dagger] \hat{\mathbf{x}} \times \mathbf{k}_{\parallel n}, \end{aligned} \quad (29)$$

and

$$\begin{aligned} \mathcal{A}_{\text{in}_n}^{(\text{TM})}[x, \omega] &= \theta(k_x^2) \sqrt{\frac{2\hbar|\omega|}{k_x^2 S}} \cos(k_x x) \\ &\times [\theta(\omega) a_{\text{in}_n}^{(\text{TM})}(k_x) - \theta(-\omega) a_{\text{in}_{-n}}^{(\text{TM})}(-k_x)^\dagger] \hat{\mathbf{x}} \times \mathbf{k}_{\parallel n}, \end{aligned} \quad (30)$$

with k_x given by Eq. (18).

By taking the output instead of the input fields, we obtain similar expressions for $\mathbf{A}_{\text{out}}^{(\text{TE})}$ and $\mathcal{A}_{\text{out}}^{(\text{TM})}$, where the input operators $a_{\text{in}_n}^{(\text{TE})}(k_x)$ and $a_{\text{in}_n}^{(\text{TM})}(k_x)$ are replaced by the output operators $a_{\text{out}_n}^{(\text{TE})}(k_x)$ and $a_{\text{out}_n}^{(\text{TM})}(k_x)$. They all satisfy the commutation relations given by Eqs. (11) and (12), and are implicitly related by the input-output transformation given by Eqs. (27) and (28). From Eqs. (27)–(30), we obtain the following result for the input-output transformation of operators:

$$\begin{aligned} a_{\text{out}_n}^{(\text{TE})}(k_x) &= a_{\text{in}_n}^{(\text{TE})}(k_x) + 2i \frac{k_x}{\sqrt{\omega_n}} \int \frac{d\omega'}{2\pi} \theta(k_x'^2) \\ &\times \sqrt{|\omega'|} \delta q[\omega_n - \omega'] \\ &\times [\theta(\omega') a_{\text{in}_n}^{(\text{TE})}(k_x') - \theta(-\omega') a_{\text{in}_{-n}}^{(\text{TE})}(-k_x')^\dagger] \end{aligned} \quad (31)$$

and

$$\begin{aligned} a_{\text{out}_n}^{(\text{TM})}(k_x) &= a_{\text{in}_n}^{(\text{TM})}(k_x) - \frac{2i}{\sqrt{\omega_n}} \int \frac{d\omega'}{2\pi} \theta(k_x'^2) \\ &\times \frac{\sqrt{|\omega'|} (k_{\parallel n}^2 - \omega_n \omega')}{|k_x'|} \delta q[\omega_n - \omega'] \\ &\times [\theta(\omega') a_{\text{in}_n}^{(\text{TM})}(k_x') - \theta(-\omega') a_{\text{in}_{-n}}^{(\text{TM})}(-k_x')^\dagger], \end{aligned} \quad (32)$$

where k_x' is related to the integration variable ω' as in Eq. (18). Within the first-order approximation considered here, Eqs (31) and (32) are fully consistent with the commutation relations of Eqs. (11) and (12).

According to Eqs. (31) and (32), the motion of the mirror may induce a mixture between creation and annihilation operators. As shown in the next section, such mixture is a signature of the effect of emission of photons out of the vacuum state.

IV. SPECTRA OF THE EMITTED PHOTONS

As a result of the motion of the mirror, the field operators are transformed according to Eqs. (31) and (32). In the representation considered here, the field state remains unchanged. We consider the simplest situation where it corresponds to the vacuum state associated to the input field operators: $|0\text{in}\rangle$. According to Eq. (10),

$$\langle 0 \text{ in} | a_{\text{out}_j}^\epsilon(k_x)^\dagger a_{\text{out}_j}^\epsilon(k_x) | 0 \text{ in} \rangle \frac{dk_x}{2\pi} \quad (33)$$

represents the average number of emitted photons with polarization ϵ (TE or TM) and wave vector \mathbf{k} with parallel component equal to $\mathbf{k}_{\parallel n}$ and x component between k_x and $k_x + dk_x$.

For the sake of simplicity, we consider a damped sinusoidal motion:

$$\delta q(t) = \delta q_0 e^{-|t|/T} \cos(\omega_0 t), \quad (34)$$

with

$$\omega_0 \delta q_0 \ll 1 \quad (35)$$

and

$$\omega_0 T \gg 1. \quad (36)$$

The first assumption corresponds to the nonrelativistic approximation, which is vital for the entire approach developed in this paper. The second assumption, on the other hand, is of secondary importance, and is taken only to avoid unnecessarily complicated results.

The matrix elements in Eq. (33) are different from zero on account of the contamination of the output annihilation (creation) operators by input creation (annihilation) operators. This also corresponds to a mixture between positive and negative frequencies, since they are, according to Eqs. (29) and (30), associated to annihilation and creation operators, respectively. In fact, the terms $a_{\text{in}_{-n}}^{(\text{TE})}(-k_x)^\dagger$ and $a_{\text{in}_{-n}}^{(\text{TM})}(-k_x)^\dagger$ in Eqs. (31) and (32) are associated to a nega-

tive input frequency ω' from which is generated an output sideband at the positive frequency $\omega_n = \omega_0 + \omega'$. From this simple reasoning, we infer that all emitted photons have frequencies ω_n in the range $\omega_n \leq \omega_0$. As a consequence, the nonrelativistic regime, Eq. (35), entails that the wavelengths λ generated out of the vacuum satisfy $\lambda \geq \delta q_0$. Actually, the long-wavelength approximation employed in this paper is equivalent to assuming the motion to be nonrelativistic and bounded, as it is the case for the example considered in Eq. (34).

A second restriction on the emitted photons originates from the plane symmetry and the corresponding conservation of the parallel component of the wave vector, $\mathbf{k}_{\parallel n}$. Since the input frequencies satisfy the inequality $-\omega' \geq k_{\parallel n}$, we have the following additional condition on the emitted photons:

$$\omega_0 - \omega_n \geq k_{\parallel n}. \quad (37)$$

We write the matrix elements in terms of the angle Θ between the x direction and the direction at which the photon is emitted:

$$\Theta = \sin^{-1}(k_{\parallel n}/\omega_n). \quad (38)$$

If $\omega_n \geq \omega_0/2$, Eq. (37) implies that no emission occurs outside the angular range defined by the inequality

$$\Theta \leq \Theta_0(\omega_n) \equiv \sin^{-1} \frac{\omega_0 - \omega_n}{\omega_n}. \quad (39)$$

Within this range, we find nonzero matrix elements from Eqs. (31)–(34):

$$\begin{aligned} & \langle 0 \text{ in } | a_{\text{out}_n}^{(\text{TE})}(k_x)^\dagger a_{\text{out}_n}^{(\text{TE})}(k_x) | 0 \text{ in } \rangle \\ &= (\delta q_0)^2 T \omega_n^2 \sqrt{\sin^2 \Theta_0 - \sin^2 \Theta} \cos^2 \Theta \end{aligned} \quad (40)$$

and

$$\begin{aligned} & \langle 0 \text{ in } | a_{\text{out}_n}^{(\text{TM})}(k_x)^\dagger a_{\text{out}_n}^{(\text{TM})}(k_x) | 0 \text{ in } \rangle \\ &= (\delta q_0)^2 T \frac{(\omega_0 - \omega_n \cos^2 \Theta)^2}{\sqrt{\sin^2 \Theta_0 - \sin^2 \Theta}}. \end{aligned} \quad (41)$$

Note that the average photon numbers do not depend on the direction of $\mathbf{k}_{\parallel n}$, as expected because of the plane symmetry. Moreover, they are proportional to the time duration of the motion T . Since we consider an open system in this paper, photon numbers are not meaningful per se, so that we must ultimately deal with photon production *rates*. For the steady oscillation considered here [see Eq. (36)], the latter should be time independent, which is in accordance with the linear time dependence in Eqs. (40) and (41). Note however that when a closed cavity system is considered, a different time dependence may result even in the case of stationary oscillations, as in the problem of an ideal cavity with resonantly oscillating boundaries, where the intracavity photon numbers may grow exponentially in time [9].

Before computing the spectra from Eqs. (40) and (41), we shall discuss an alternative approach based on the effective Hamiltonian [2]

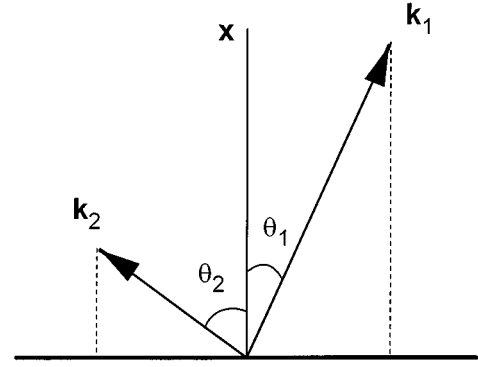


FIG. 1. Twin photons emitted at the directions indicated by the angles θ_1 and θ_2 , with wave vectors \mathbf{k}_1 and \mathbf{k}_2 . Note that $\mathbf{k}_{1\parallel} = -\mathbf{k}_{2\parallel}$ (see text).

$$\delta H = -\delta q(t)F, \quad (42)$$

where F is the field operator representing the force exerted on the mirror along the x direction. Since it is a quadratic operator on the field, δH is formally analogous to the Hamiltonian describing photon pair creation by parametric interaction of a classical pump wave at frequency ω_0 with a $\chi^{(2)}$ nonlinear medium. Therefore, we may expect that the motional effect leads to the emission of pair of photons at frequencies ω_1 and ω_2 such that

$$\omega_1 + \omega_2 = \omega_0. \quad (43)$$

Furthermore, the two photons have the same polarization and wave vectors \mathbf{k}_1 and \mathbf{k}_2 such that

$$\mathbf{k}_{1\parallel} + \mathbf{k}_{2\parallel} = \mathbf{0}, \quad (44)$$

on account of the translational symmetry along the plane of the mirror. In Fig. 1, we represent the two wave vectors and their angles Θ_1 and Θ_2 with the x direction. According to Eq. (44), they are related by the equation

$$\omega_1 \sin \Theta_1 = \omega_2 \sin \Theta_2. \quad (45)$$

Equation (43) shows again that the emitted photons have frequencies smaller than ω_0 . Let us take ω_1 to be the largest frequency in the pair, $\omega_0 \geq \omega_1 \geq \omega_0/2$. Then, Eq. (45) entails that the low-frequency photon is emitted along a direction further from the x direction: $\Theta_2 > \Theta_1$. As Θ_1 increases from zero to its maximum value $\Theta_0(\omega_1)$ given by Eq. (39), Θ_2 varies from zero to $\pi/2$.

Although the approach based on Eq. (42) is useful for the interpretation of the results obtained in this paper, it is not strictly consistent with our model of perfectly reflecting moving mirrors. In fact, no Hamiltonian description is available in this case [13]. Nevertheless, this effective model correctly describes the physics of perfectly reflecting moving mirrors — including the connection between fluctuations and dissipation [2,12,15] — because it loosely corresponds to the model of a dielectric mirror (whose interaction with the field may be described by a Hamiltonian model [11]) in the limit of large refraction index (yet according to a recent calcula-

tion, an unexpected effect occurs when taking this limit in 3D space, namely, the emission of photons inwards into the medium [8].

In order to compute the photon spectra from Eqs. (40) and (41), we first consider the number of photons $dN^\epsilon(\mathbf{k})$ emitted with polarization ϵ and wavevector \mathbf{k} inside a volume d^3k in reciprocal space. Since we have employed periodic boundary conditions over the mirror's surface S in the two-dimensional yz reciprocal space [see Eq. (6)], we multiply the expression in Eq. (33) by the number of cells in the yz reciprocal space to find

$$dN^\epsilon(\mathbf{k}) = \langle 0 | \text{in} | a_{\text{out}_j}^\epsilon(k_x)^\dagger a_{\text{out}_j}^\epsilon(k_x) | 0 \text{in} \rangle \frac{d^3k}{(2\pi)^3} S. \quad (46)$$

By taking polar coordinates in the 3D reciprocal space, we obtain from Eq. (46) the number of photons with polarization ϵ per unit frequency interval and solid angle (denoted as Ω):

$$\frac{dN^\epsilon}{d\omega d\Omega}(\omega, \Theta) = S \frac{\omega^2}{(2\pi)^3} \langle 0 | \text{in} | a_{\text{out}_j}^\epsilon(k_x)^\dagger a_{\text{out}_j}^\epsilon(k_x) | 0 \text{in} \rangle. \quad (47)$$

We express the number of photons at a given frequency ω_1 and angle Θ_1 in terms of the frequency ω_2 and the angular coordinate Θ_2 of the accompanying emitted photon ("idle" or "twin" photon), which are given by Eqs. (43) and (45), respectively. From Eqs. (40) and (47) we derive the angular spectrum for TE polarization:

$$\frac{dN}{d\omega d\Omega}^{(\text{TE})}(\omega_1, \Theta_1) = T \frac{S}{(2\pi)^3} (\delta q_0)^2 \omega_1^3 \omega_2 \cos^2 \Theta_1 \cos \Theta_2. \quad (48)$$

For TM photons, Eqs. (41) and (47) yield

$$\begin{aligned} \frac{dN}{d\omega d\Omega}^{(\text{TM})}(\omega_1, \Theta_1) \\ = T \frac{S}{(2\pi)^3} (\delta q_0)^2 \omega_1^3 \omega_2 \frac{(1 + \sin \Theta_1 \sin \Theta_2)^2}{\cos \Theta_2}. \end{aligned} \quad (49)$$

The angular spectra as given by Eqs. (48) and (49) are both proportional to the mirror's surface S as expected.

Since the photons are created in pairs, to each photon emitted at frequency ω_1 along the direction Θ_1 there is an idle photon of frequency ω_2 emitted along the direction Θ_2 . As a consequence, the angular spectra must satisfy

$$\begin{aligned} \frac{dN^\epsilon}{d\omega d\Omega}(\omega_1, \Theta_1) \sin \Theta_1 d\Theta_1 |d\omega_1| \\ = \frac{dN^\epsilon}{d\omega d\Omega}(\omega_2, \Theta_2) \sin \Theta_2 d\Theta_2 |d\omega_2|. \end{aligned} \quad (50)$$

In order to show that the results in Eqs. (48) and (49) agree with Eq. (50), we write

$$\sin \Theta_1 d\Theta_1 = \left(\frac{\omega_2}{\omega_1} \right)^2 \frac{\cos \Theta_2}{\cos \Theta_1} \sin \Theta_2 d\Theta_2, \quad (51)$$

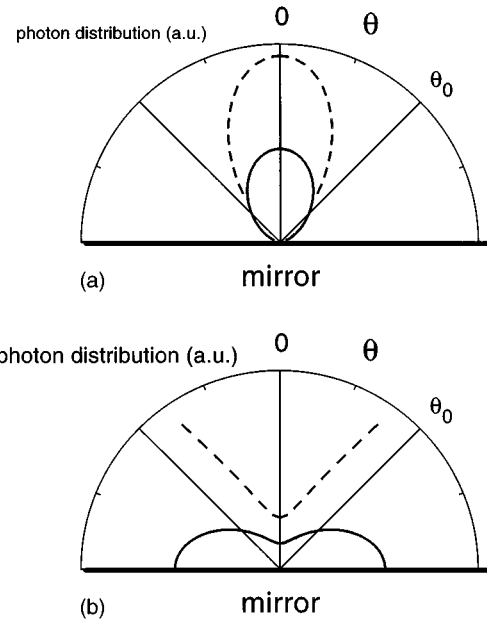


FIG. 2. Polar diagrams representing the angular distributions for photon emission as functions of the emission angle Θ and for a fixed photon frequency ω . The direction corresponding to $\Theta=0$ is perpendicular to the surface of the mirror. We employ different scales to represent TE (a) and TM (b) polarizations. The dashed lines correspond to $\omega=(2-\sqrt{2})\omega_0$ (then yielding $\Theta_0=\pi/4$), whereas the solid lines correspond to $\omega=(\sqrt{2}-1)\omega_0$. Accordingly, dashed and solid curves represent the angular distributions for "signal" and "idle" photons which constitute a given pair created out of the vacuum state, since the two frequencies considered are such that their sum equals the mechanical frequency ω_0 . When integrated over the solid angle, the dashed and solid lines for each polarization provide the same (polarization dependent) spectral distributions (see Fig. 3).

which follows from Eq. (45), and $d\omega_1 = -d\omega_2$, which follows from Eqs. (43).

When considering propagation along the normal to the surface of the mirror, TE and TM polarizations become rigorously equivalent. In accordance with this property, Eqs. (48) and (49) provide identical results for the photon distributions at the forward direction $\Theta_1(=\Theta_2)=0$. However, they behave very differently at larger angles. In Fig. 2(a), we plot the TE angular photon distributions $dN^{(\text{TE})}(\omega_1, \Theta_1)/d\omega d\Omega$ as given by Eq. (48) with $\omega_1=(2-\sqrt{2})\omega_0$ (dashed line) as well as $dN^{(\text{TE})}(\omega_2, \Theta_2)/d\omega d\Omega$ with $\omega_2=\omega_0-\omega_1=(\sqrt{2}-1)\omega_0$ (solid line). Note that TE photons are loosely concentrated near the forward direction. On the other hand, the angular distribution for TM polarization is minimum at the forward direction as illustrated in Fig. 2(b), where we plot $dN^{(\text{TM})}(\omega_1, \Theta_1)/d\omega d\Omega$ (dashed line) and $dN^{(\text{TM})}(\omega_2, \Theta_2)/d\omega d\Omega$ (solid line) for the same values of ω_1 and ω_2 considered in Fig. 2(a). High-frequency TM photons are mostly emitted into a rather narrow angular sector bounded by the angle $\Theta_0(\omega_1)$ (which is equal to $\pi/4$ in the numerical example considered in Fig. 2). As a matter of fact, the angular spectrum of TM photons as given by Eq. (49) diverges at $\Theta_1=\Theta_0(\omega)$, since this corresponds to the situation where the idle photon is emitted along the grazing direction: $\Theta_2=\pi/2$. Such singular behavior results from the

effect of resonant excitation of surface TM waves induced by the motion [14]. Note, however, that $dN^{(\text{TM})}(\omega_2, \Theta_2)/d\omega d\Omega$ is finite as $\Theta_2 \rightarrow \pi/2$, because the corresponding solid angle $2\pi \sin\Theta_2 d\Theta_2$ as given by Eq. (51) also becomes very large in this limit. In other words, for each (low-frequency) TM photon emitted over a broad angular sector near the grazing direction, its (high-frequency) ‘‘twin’’ is emitted into a narrow angular sector close to and bounded by Θ_0 .

We may obtain the frequency spectra from Eqs. (48) and (49) by integrating the angular spectra over the solid angle Ω . We obtain simpler results by taking the dimensionless variable

$$\Delta = 2\frac{\omega}{\omega_0} - 1,$$

representing the difference between the two frequencies associated to a given pair of photons. For TE polarization we find

$$\frac{dN^{(\text{TE})}}{d\omega}(\omega) = T \frac{S}{64\pi^2} (\delta q_0)^2 \omega_0^4 \left[\frac{1}{4}(1 - \Delta^4) + \Delta^2 \log|\Delta| \right]. \quad (52)$$

The result for TM polarization is

$$\begin{aligned} \frac{dN^{(\text{TM})}}{d\omega}(\omega) = & -T \frac{S}{64\pi^2} (\delta q_0)^2 \omega_0^4 \\ & \times \left[\frac{1}{4}(7 - 8\Delta^2 + \Delta^4) + (2 + \Delta^2) \log|\Delta| \right]. \end{aligned} \quad (53)$$

Both $dN^{(\text{TE})}/d\omega$ and $dN^{(\text{TM})}/d\omega$ are even functions of Δ , hence implying that

$$\frac{dN^\epsilon}{d\omega}(\omega) = \frac{dN^\epsilon}{d\omega}(\omega_0 - \omega). \quad (54)$$

This is again a signature of generation of twin photons with frequencies given by Eq. (43), as in a parametric process with a classical pump field of frequency ω_0 .

In Fig. 3, we plot $dN^{(\text{TE})}/d\omega$ and $dN^{(\text{TM})}/d\omega$ as functions of ω/ω_0 . As expected the plots are symmetric with respect to the axis $\omega/\omega_0 = 1/2$. According to Eq. (53) and as displayed in Fig. 3, the TM spectrum has a logarithmic divergence at $\omega/\omega_0 = 1/2$, a residue of the singular behavior of the angular spectrum as $\Theta \rightarrow \Theta_0$. In fact, $\omega_0/2$ is a unique frequency in the sense that both twin photons may be emitted along the grazing direction — as shown by Eq. (39), $\Theta_0 = \pi/2$ in this case.

The total number of emitted photons is derived from the spectra given by Eqs. (52) and (53). We find that TM photons are produced in a larger number than TE photons:

$$N^{(\text{TM})} = 11N^{(\text{TE})} = \frac{11}{720\pi^2} TS (\delta q_0)^2 \omega_0^5. \quad (55)$$

As a consequence of the symmetry expressed by Eq. (54), the total radiated energy is given by

$$E = (N^{(\text{TE})} + N^{(\text{TM})}) \hbar \omega_0 / 2. \quad (56)$$

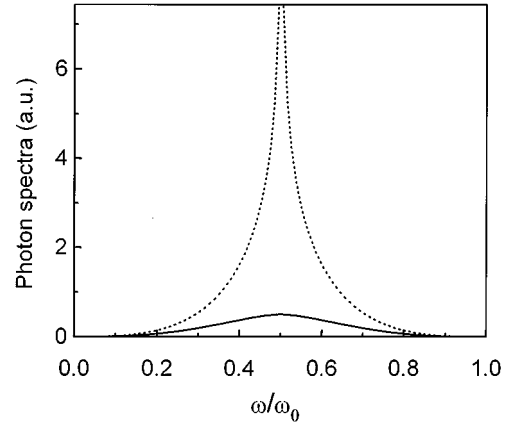


FIG. 3. Frequency spectra of TE (solid line) and TM (dashed line) photons as functions of ω/ω_0 . They are symmetric with respect to the value $\omega/\omega_0 = 1/2$. Note that the TM spectrum diverges at this value.

The total radiated energy is directly related to the dissipative force $F(t)$ exerted on the mirror, which was derived in Ref. [3]. For the particular motion given by Eq. (34), it reads

$$F(t) = \frac{\hbar}{60\pi^2} S \omega_0^5 \delta q_0 e^{-|t|/T} \sin(\omega_0 t). \quad (57)$$

Then Eqs. (34) and (55)–(57) yield

$$E = - \int dt F(t) \delta \dot{q}(t), \quad (58)$$

in agreement with energy conservation.

V. DISCUSSION AND CONCLUSION

From Eq. (55) we may obtain the total photon production rate, which is written in terms of the maximum value of the mirror’s velocity $v_{\text{max}} = \omega_0 \delta q_0$ and the length $\lambda_0 = 2\pi c/\omega_0$ (which is smaller and of the order of the wavelengths generated by the motion) so as to allow for a direct comparison with the 1D result of Ref. [6]:

$$\frac{N}{T} = \frac{1}{15} \frac{S}{\lambda_0^2} \left(\frac{v_{\text{max}}}{c} \right)^2 \omega_0, \quad (59)$$

where we have reintroduced the constant c in order to provide an explicit evaluation of the orders of magnitude. As compared to the 1D result, the 3D production rate contains an extra ‘‘geometrical’’ factor equal to S/λ_0^2 , as already surmised in Ref. [6]. Note that we have considered from the start an infinite plane mirror, which actually describes the limit $S/\lambda_0^2 \gg 1$ (see Ref. [12] for a detailed discussion on how such limit is obtained from the general case of a finite-size time-dependent deformation of a plane mirror). On the other hand, when $S/\lambda_0^2 \sim 1$, diffraction at the boundaries of the mirror play an important role, then resulting in a different dependence on S . For the presently available mechanical frequencies, λ_0 is at least in the centimeter range. Therefore, we believe that a calculation taking into account diffraction due to the mirror’s finite size would be necessary for the quanti-

tative description of an experiment aimed to observe quantum radiation by moving mirrors. Nevertheless, a rough estimate of the photon production rate may be obtained from Eq. (59) by taking $S/\lambda_0^2 \sim 1$, $\omega_0/(2\pi) \sim 10$ GHz and $v_{\max}/c \sim 10^{-7}$, then yielding $N/T \sim 10^{-5}$ photons/sec. This shows that quantum radiation by a single moving mirror is a very small effect.

In conclusion, we have obtained the angular and frequency distributions of the photons created out of the electromagnetic vacuum state when a plane mirror oscillates in the nonrelativistic regime. TM-polarized photons are created at a larger rate than TE photons, except when measuring at the direction perpendicular to the mirror's surface, where the production rates are equal. TE and TM angular distributions are respectively maximum and minimum at this direction. TM photons with frequencies larger than $\omega_0/2$ (high-frequency photons) are mostly emitted along directions at angles close to and smaller than the frequency-dependent angle Θ_0 defined by Eq. (39), which is also an upper bound for the angular directions of emission of high frequency photons for both polarizations. As the photon frequency ω approaches its maximum allowed value — given by the me-

chanical frequency ω_0 , Θ_0 tends to zero, and thereby the angular distributions become very narrow. Most photons, however, are emitted at frequencies near $\omega_0/2$, and hence over a broad angular range, since $\Theta_0 = \pi/2$ in this case. Low-frequency TM photons are preferably emitted at directions not far from the grazing direction.

Unlike the Hamiltonian approach developed in Refs. [7,11], our method does not explicitly unveil the two-photon nature of the emission process. However, the symmetry properties of the spectra obtained in this paper clearly indicate that the photons are emitted in pairs, the “twin” photons having identical polarizations, opposite momenta along the plane of the mirror, and frequencies that add to give ω_0 .

ACKNOWLEDGMENTS

We thank A. Lambrecht, M.-T. Jaekel, and S. Reynaud for discussions. This work was partially supported by the Conselho Nacional de Desenvolvimento Científico e Tecnológico and by the Fundação de Amparo à Pesquisa do Estado do Rio de Janeiro.

-
- [1] L. H. Ford and A. Vilenkin, *Phys. Rev. D* **25**, 2569 (1982).
 [2] M. T. Jaekel and S. Reynaud, *Quantum Opt.* **4**, 39 (1992); *J. Phys. (France) I* **2**, 149 (1992).
 [3] P. A. Maia Neto, *J. Phys. A* **27**, 2167 (1994).
 [4] V. V. Dodonov and A. B. Klimov, *Phys. Lett. A* **167**, 309 (1992).
 [5] C. K. Law, *Phys. Rev. A* **49**, 433 (1994).
 [6] A. Lambrecht, M.-T. Jaekel, and S. Reynaud, *Phys. Rev. Lett.* **77**, 615 (1996).
 [7] G. Barton, *Ann. Phys. (N.Y.)* **245**, 361 (1996).
 [8] G. Barton and C. A. North (unpublished).
 [9] V. V. Dodonov and A. B. Klimov, *Phys. Rev. A* **53**, 2664 (1996).
 [10] C. Eberlein, *Phys. Rev. A* **53**, 2772 (1996); *Phys. Rev. Lett.* **76**, 3842 (1996).
 [11] G. Barton and C. Eberlein, *Ann. Phys. (N.Y.)* **227**, 222 (1993).
 [12] P. A. Maia Neto and L. A. S. Machado, *Brazilian J. Phys.* **25**, 324 (1995).
 [13] G. T. Moore, *J. Math. Phys.* **11**, 2679 (1970).
 [14] P. A. Maia Neto, *Opt. Commun.* **105**, 151 (1994).
 [15] G. Barton, in *Cavity Quantum Electrodynamics*, edited by P. Berman, supplement to *Adv. At. Mol. Opt. Phys.* (1993); V. B. Braginsky and F. Ya. Khalili, *Phys. Lett. A* **161**, 197 (1991); P. A. Maia Neto and S. Reynaud, *Phys. Rev. A* **47**, 1639 (1993).